

1 **Fig. S1** Characterization of GO. XRD patterns (A), FT-IR spectrum (B), High
2 resolution XPS spectrum for C 1s peak (C) and O 1s peak (D).

3 **Fig. S2** (A) AFM image of the GO nanosheets, (B) The corresponding AFM height
4 image.

5 **Fig. S3** Concentrations of the residual GO nanosheets in the supernatant as a function
6 of different concentrations of *E. Coli* and *S. Aureus*.

7 **Fig. S4** Concentrations of RNA of *E. Coli* and *S. Aureus* in the PBS as a function of
8 GO concentration.

9 **Fig. S5** FT-IR spectra of GO (1), GO-LMH (2), GO-CPC (3), and GO-GMS (4).

10 **Fig. S6** Adsorption isotherms of LMH, CPC and GMS on GO. pH = 7.0 ± 0.1 , m/V =
11 60 mg/L.

12

13 **Table S1** Chemical structures and selected physicochemical properties of LMH, CPC
14 and GMS.

15 **Table S2** Optimized adsorption energies (E_{ad}) of three antibiotics on GO.

16 **Table S3** Comparison of the inhibition of different adding orders under the same
17 experimental condition.

18 **Table S4** Curve fitting results of XPS C 1s spectra.

19 **Table S5** Curve fitting results of XPS O 1s spectra.

20

21 **Bacterial cultivation and inactivation experiments**

22 The bacteria were cultured in Luria-Bertani (LB) broth (containing 5 g/L of Yeast
23 extract, 10 g/L of Tryptone and 5 g/L of NaCl) overnight with the rotation speed of
24 150 rpm at 37 °C until they reached the logarithmic growth phase. The bacteria in the
25 vegetative state were harvested via centrifugation at 8000 rpm for 10 min. After
26 removing the supernatant, the bacteria were re-suspended in the sterile normal saline
27 (9 g/ L NaCl) and then centrifuged again at 8000 rpm for 10 min. This washing step
28 was repeated once. The stock concentrations of *E. coli* and *S. aureus* were diluted and
29 injected into sterile normal saline to reach a final volume of 5 ml with concentrations
30 of nearly 1×10^8 to 1×10^9 colony forming units (CFU)/mL. The number of viable

1 microorganisms was estimated by the plate count method.

2 For the inactivation experiments, all required reagents were added into 10 mL a
3 culture tube to obtain the desired concentration. The assessments were carried out
4 under anaerobic conditions with the culture tubes sealed at 37 °C (the optimum
5 temperature). The sealed culture tubes were put on a shaking incubator at 150 rpm for
6 2 h. Then the treated bacterial solution was serially tenfold diluted with sterile normal
7 saline and 100 µL of diluted bacterial solution to be plated, incubated at 37 °C for 18
8 h, and then counted. The inhibited numbers of *E. coli* and *S. aureus* were calculated
9 from the difference between the initial numbers (N_0) and the remaining ones after
10 inactivation experiments (N_t , t: interaction time). The antibacterial activity was
11 expressed as follows:

$$12 \quad Inhibition(\%) = \frac{N_0 - N_t}{N_0} \times 100\%$$

13

14 **Bacterial cell membrane integrity assessment**

15 In detail, bacterial cell suspension with different concentration of GO (10 or 40 mg/L)
16 were added into individual wells of a 24-well microplate (Greiner) and placed on a
17 shaking incubator at 150 rpm for 2 h. Then, 10 µL of mixture DNA dyes (SYTO9:PI
18 = 1:1) was added into the bacterial cell and GO suspension solution. The mixed
19 solution was then dyed in the dark at room temperature for 15 min. The cell
20 membrane integrity of bacterial was visualized by laser scanning confocal microscope
21 (Auriga, Zeiss, Germany) qualitatively. With the excitation wavelength centered at
22 about 485 nm for SYTO9 and PI, measure the fluorescence intensity at wavelengths
23 centered at about 530 nm (green) and 630 nm (red), respectively. Different green-to-
24 red fluorescence intensity ratio was proportional to different percentage of bacterial
25 with intact-to-damaged cell membranes.

26

27 **DFT calculations**

28 The convergence of plane-wave expansion was obtained with a cut-off energy of 400
29 eV. The GO model is built by cell parameters of $a = b = c = 15 \text{ \AA}$; $\alpha = \beta = \gamma = 90^\circ$.

1 The 3D structure data of three antibiotics came from ChemSpider
2 (<http://www.chemspider.com>). The k-point meshes in the Brillouin zone (BZ) were
3 sampled by $3 \times 3 \times 3$. All structures were optimized until the forces on all
4 unconstrained atoms were less than 0.02 eV/\AA .

5 The adsorption energy (E_{ad}) of the three antibiotics molecule was calculated as

$$6 \quad E_{\text{ad}} = E_{\text{GO}} + E_{\text{antibiotic}} - E_{\text{antibiotic/GO}}$$

7 where E_{GO} is the energy of GO surface; $E_{\text{antibiotic}}$ is the energy of antibiotic
8 molecules; and $E_{\text{antibiotic/GO}}$ is the total energy of the antibiotic molecule sorbed on the
9 GO surface. A positive E_{ad} value implies a stable sorption.

10

11 **Characterization of GO**

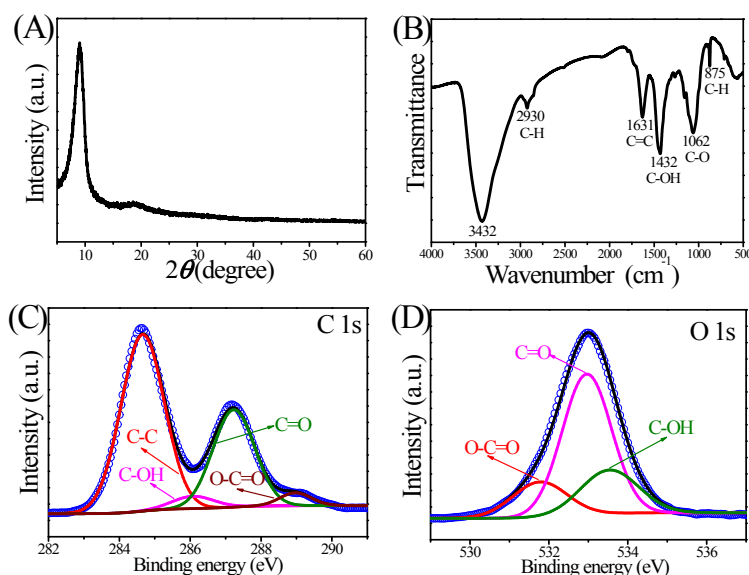
12 The XRD pattern of the GO was obtained from a D/Max-rB equipped with a rotation
13 anode using Cu $K\alpha$ radiation ($\lambda = 1.5418 \text{ nm}$) at 40 kV and 200 mA. The XRD
14 patterns of GO (Fig. S1A) exhibits a diffraction peak at $2\theta = 9.02^\circ$ with a d -spacing of
15 0.98 nm , corresponding to the characteristic diffraction pattern of GO.

16 The sample for the FT-IR measurement was mounted on a BrukerEquinox55
17 spectrometer (Nexus) in KBr pellet at room temperature. Fig. S1B shows the FT-IR
18 spectra of GO. The broad band at 3432 cm^{-1} corresponds to the presence of associated
19 and free hydroxyl groups due to structural hydroxyl groups ($-\text{COOH}$ and $-\text{COH}$) of
20 GO and intercalated water. The bands at 2930, 1631, 1432, 1062 and 875 cm^{-1} are
21 attributed to C–H, aromatic C=C, C–OH, C–O and C–H stretching vibrations,
22 respectively, indicating that large amounts of oxygen-containing functional groups
23 such as carboxyl, carbonyl, and hydroxyl groups are present on GO surface.

24 The chemical composition and the element characterization of GO was measured by
25 X-ray photoelectron spectroscopy (XPS). XPS measurement was performed in a VG
26 Scientific ESCALAB Mark II spectrometer equipped with two ultrahigh vacuum
27 chambers. The high-resolution C 1s and O 1s spectra of GO are presented in Fig.S1C
28 and 1D, respectively. The C 1s peak can be decomposed into four components (Fig.
29 S1C and Table S4). The peaks at 284.66 eV correspond to C–C bonds and its content
30 is 60.67%. The peaks located approximately at 286.08 (4.06%), 287.23 (32.08%) and

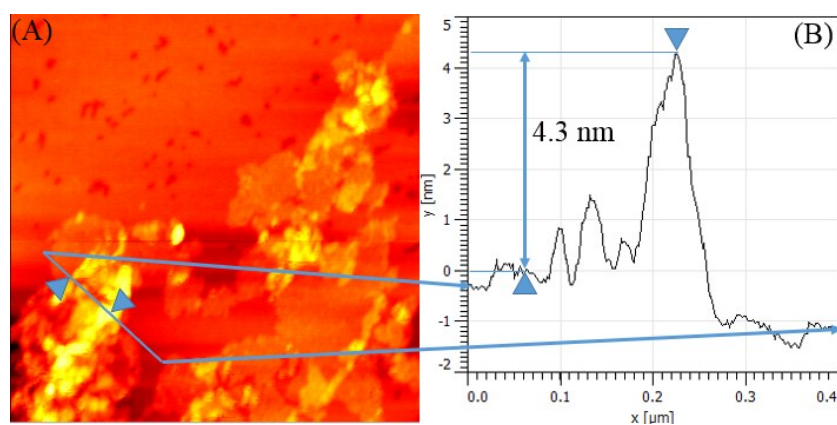
1 288.97 (3.19%) eV are the C-OH, C=O and O-C=O bonds, respectively. As shown in
 2 Fig. S1D and Table S5, the O 1s peak can be decomposed into three components. The
 3 content of C=O bond (at 532.96 eV) takes up 60.68%, which demonstrate that oxygen
 4 atom of GO exist in C=O bond dominantly. The peaks at 531.78 (17.09%) and 533.53
 5 (22.22%) eV are assigned to the O-C=O band and the C-OH bond, respectively.
 6 Based on the elemental compositions of GO determined by XPS, the ratio of carbon
 7 to oxygen (C/O) is about 2.88 in GO, which is consistent with the previous study
 8 reported that the C/O ratio of GO prepared by Hummer's method is in the range of 2–
 9 3. The content of O is 25.79 %, suggesting the considerable degree of oxidation of the
 10 synthesized GO by the oxidant.

11 The atomic force microscopy (AFM) images were obtained in air using a Digital
 12 Instrumental Nanoscope III in tapping mode to measure the thickness of the
 13 synthesized GO nanosheets. The results were presented in Fig.S2A. The height image
 14 shown in Fig.S2B indicates that the thickness of the GO sheets varies between 3 and 5
 15 nm, corresponding to approximately 3-5 layers.



16
 17 **Fig. S1** Characterization of GO. XRD patterns (A), FT-IR spectrum (B), High
 18 resolution XPS spectrum for C 1s peak (C) and O 1s peak (D).

19



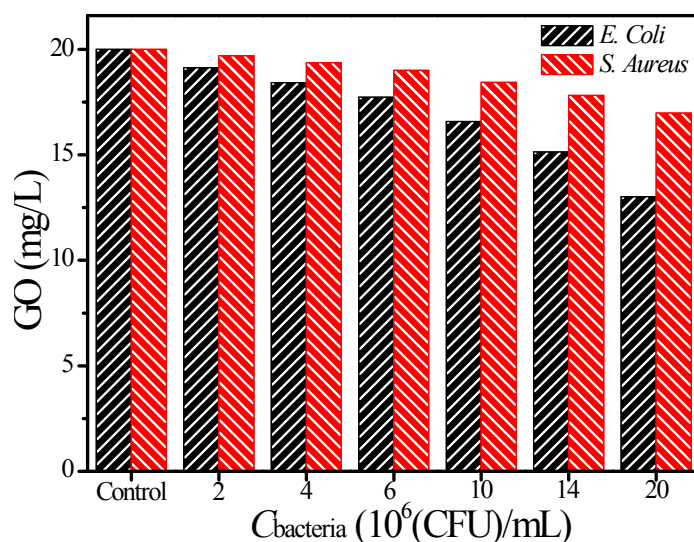
1

2 **Fig. S2** (A) AFM image of the GO nanosheets, (B) The corresponding AFM height
 3 image.

4

5 **The adhesion of GO on bacteria**

6 In order to further find proof of the GO adhesion, the concentrations of the residual
 7 GO nanosheets in the supernatant as a function of different concentrations of *E. Coli*
 8 and *S. Aureus* were measured. In details: GO (20 mg/L) after treated with different
 9 concentrations of *E. Coli* and *S. Aureus* for 2 h. Then the bacteria were separated from
 10 solution by centrifugation at 5000 rpm for 5 min (In the absence of bacteria, the
 11 concentration of GO in the solution was not changed by centrifugation at 5000 rpm
 12 for 5 min). The concentrations of the residual GO nanosheets in the supernatant were
 13 determined by UV-vis spectrophotometer (UV-2550, PerkinElmer) at a wavelength of
 14 227 nm. The corresponding results were shown in Fig. S3. One can see that the
 15 concentrations of the residual GO nanosheets in the supernatant decrease as the
 16 concentrations of *E. Coli* and *S. Aureus* increase, indicating some GO nanosheets can
 17 attach on bacteria.



1

2 **Fig. S3** Concentrations of the residual GO nanosheets in the supernatant as a function
 3 of different concentrations of *E. Coli* and *S. Aureus*.

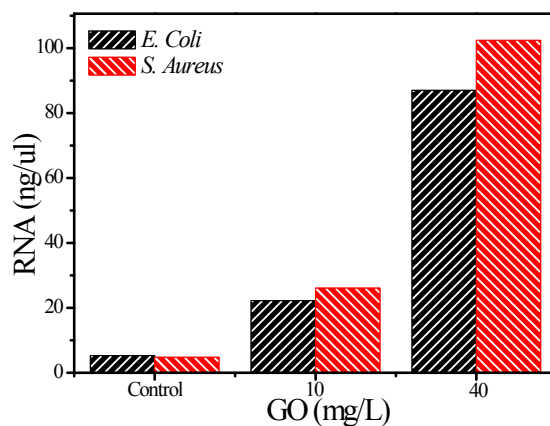
4

5 **The concentration of RNA in the supernatant.**

6 Firstly, the phosphate buffer solution (PBS) remaining from the antibacterial test of
 7 each sample was diluted to 5 mL. Then, the solution was centrifuged at 2000 rpm for
 8 10 min. After that, a vial tube with 5 μL of β -mercaptoethanol was loaded by 1 mL of
 9 the supernatant of the solution. RNA of the bacteria was separated using a RNA
 10 purification kit and measured with a NanoDrop 2000C spectrophotometer (Thermo,
 11 USA).

12 The toxicity of GO to bacteria through cell membrane damage can be investigated by
 13 measuring the intracellular materials of the bacteria in the PBS after exposed to GO.
 14 Concerning this, the efflux of cytoplasmic materials of the broken *E. coli* and *S.*
 15 *aureus* bacteria is evaluated by determining the concentration of RNA in the solution
 16 as shown in Fig. S4. When exposed to the GO nanosheets, the RNA concentrations of
 17 the bacteria in the solution are obviously higher than those of control samples,
 18 indicating the contact of bacteria with GO causes the damage to cell membrane. The
 19 increases in concentration of RNA in the solution demonstrate that GO can damage
 20 the bacterial cell membrane and the destructive power increase with increasing GO
 21 concentration. Fig. S4 also shows that the effluxes of RNA from *S. aureus* exposed to
 22 GO are higher than those from *E. coli*, indicating that GO shows more bactericidal

1 efficiency toward *S. aureus* than toward *E. coli*, consistent with the results of
2 inactivation experiment.



3

4 **Fig. S4** Concentrations of RNA of *E. Coli* and *S. Aureus* in the PBS as a function of
5 GO concentration.

6

7 **Method description of the studies of GO-antibiotics interaction by UV-vis** 8 **spectrophotometer and Nanosizer ZS instrument**

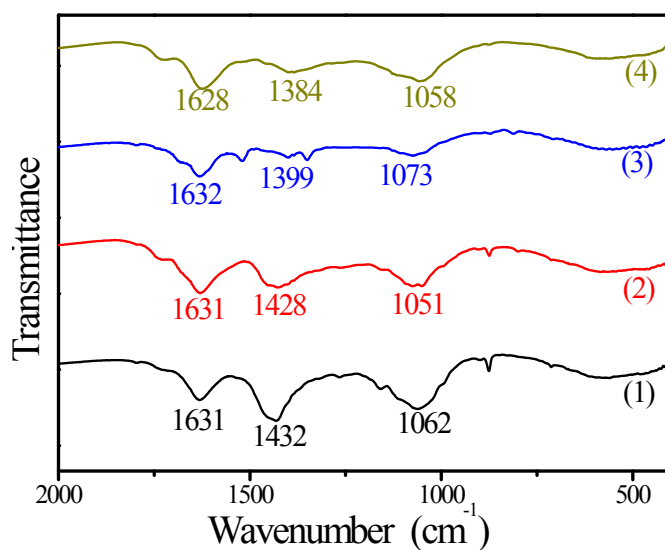
9 The volumes of GO stock suspension, the stock solutions of the antibiotics and Milli-
10 Q water were added to the glass vials to achieve the desired concentrations of
11 different components. The desired initial pH values of the suspension in each glass
12 vial were adjusted by adding negligible amounts of HCl or NaOH. The glass vials
13 containing these mixtures were placed on a horizontal shaker and shaken at a constant
14 speed of 150 rpm for 2 h. Then the samples were studied by UV-vis
15 spectrophotometer (UV-2550, PerkinElmer) and Nanosizer ZS instrument (Malvern
16 Instrument Co. Worcestershire, UK). For the UV-vis determination, the reference
17 sample is Milli-Q water.

18

19 **FT-IR spectrum analysis of the interaction of GO and antibiotics**

20 The FT-IR spectra of GO in the absence and presence of antibiotics were shown in
21 Fig. S5. In the absence of antibiotics, the characteristic peaks of GO located at 1062
22 (C-O), 1432 (O-C=O), and 1631 (C=C) cm^{-1} are observed. The band at 1631 cm^{-1}
23 assigned to bending vibration of C=C on GO shifts to 1628 cm^{-1} after interaction with

1 GMS. . The band at 1432 cm^{-1} assigned to bending vibration of C–OH on GO shifts
2 to 1428 , 1399 and 1384 cm^{-1} after interaction with LMH, CPC and GMS, respectively.
3 And the band at 1062 cm^{-1} assigned to bending vibration of C–O on GO shifts to
4 1051 , 1073 and 1058 cm^{-1} after interaction with LMH, CPC and GMS, respectively.
5 In the presence of antibiotics, the positions and intensities of the characteristic peaks
6 of GO are changed (Fig. S5), which supports the adsorption of antibiotics on GO with
7 different mechanisms. CPC with one aromatic structure and nitro group can be
8 adsorbed on GO via π – π coupling/stacking and π – π EDA interaction. LMH without
9 aromatic ring structure and π –electron–acceptor functional groups can be adsorbed on
10 GO via nonelectrostatic interactions including van der Waals forces and H-bonding
11 rather than π – π EDA. GMS can be adsorbed on GO by cation– π bonding interaction
12 between protonated amino groups of GMS and π electron-rich structures of GO.



13

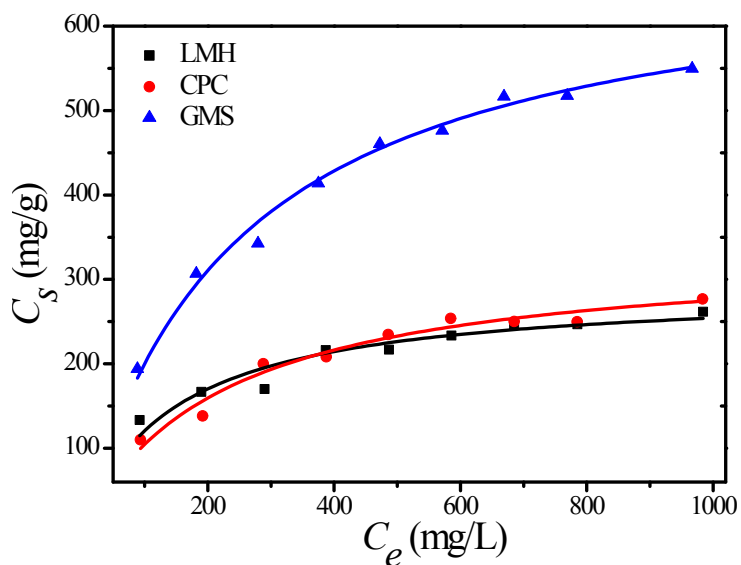
14 **Fig. S5** FT-IR spectra of GO (1), GO-LMH (2), GO-CPC (3), and GO-GMS (4).

15

16 **Adsorption of antibiotics on GO**

17 The volumes of GO stock suspensions and stock solution of antibiotics were added
18 into the polyethylene tubes to achieve the desired concentrations of the different
19 components. The pH of the solutions was adjusted by adding negligible volumes of
20 0.1 or 0.01 mol/L HCl or NaOH solutions. After shaken for 24 h, the suspension was
21 centrifuged at 20,000 rpm for 30 min. Then the supernatant was filtered by using

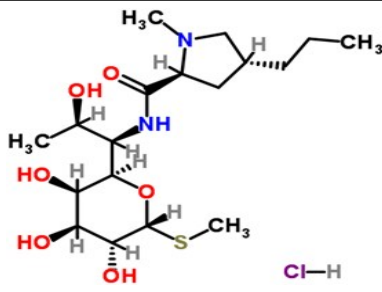
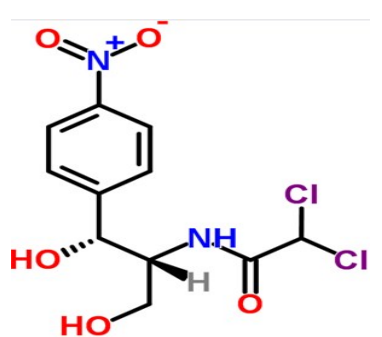
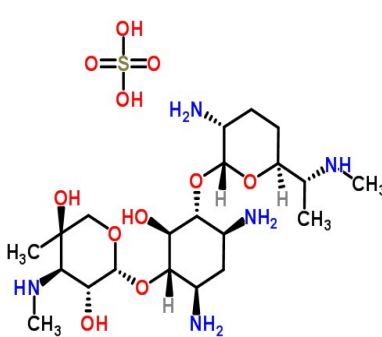
1 0.22- μm membrane filters. The supernatant was collected for determination the
2 concentrations of LMH, CPC and GMS by UV-vis absorbance using a calibration
3 curve built with different concentrations of antibiotic solutions at 214, 278 and 200
4 nm, respectively. Fig. S6 shows adsorption isotherms of LMH, CPC and GMS on GO
5 nanosheets. The maximum adsorption capacities of GO ($C_{s\text{max}}$) calculated by
6 Langmuir model are 303.03 mg/g for LMH, 335.85 mg/g for CPC and 666.67 mg/g
7 for GMS.



8
9 **Fig. S6** Adsorption isotherms of LMH, CPC and GMS on GO. $\text{pH} = 7.0 \pm 0.1$, $\text{m/V} =$
10 60 mg/L.

11
12
13
14
15
16
17
18
19
20

1 **Table S1** Chemical structures and selected physicochemical properties of LMH, CPC
2 and GMS.

Antibiotic	Molecular structure	Physicochemical properties	
Lincomycin hydrochloride		Molecular Formula	C ₁₈ H ₃₄ N ₂ O ₆ ·HCl
		Molecular weight	443.00
		pK _a	7.60
		log K _{ow}	0.20
		Water solubility	927 mg/L (25°C)
Density	1.08		
Chloramphenicol		Molecular Formula	C ₁₁ H ₁₂ Cl ₂ N ₂ O ₅
		Molecular weight	323.13
		pK _a	11.03
		log K _{ow}	1.14
		Water solubility	2500 mg/L (25°C)
Density	1.55		
Specific rotation	19.5°		
Gentamycin Sulfate		Molecular Formula	C ₂₁ H ₄₃ N ₅ O ₇ ·H ₂ SO ₄
		Molecular weight	575.67
		C1(25-50%)	C ₂₁ H ₄₃ N ₅ O ₇
		C2(25-55%)	C ₂₀ H ₄₁ N ₅ O ₇
		C3(10-35%)	C ₁₉ H ₃₉ N ₅ O ₇
		Specific rotation	107-121°
Water solubility	50 g/L (25°C)		

3

4 **Table S2** Optimized adsorption energies (E_{ad}) of three antibiotics on GO.

Samples	E_{GO}	$E_{antibiotic}$	$E_{antibiotic/GO}$	E_{ad}
GO+LMH	-470.75	-372.95	-845.42	1.71
GO+CPC	-470.75	-210.55	-683.09	1.79
GO+GMS	-470.75	-465.60	-938.62	2.27

5

6

1 **Table S3** Comparison of the inhibition of different adding orders under the same
 2 experimental condition.

Adding ways	<i>E. Coli</i>			<i>S. Aureus</i>		
	LMH	CPC	GMS	LMH	CPC	GMS
(B+A)	20.0%	55.7%	99.8%	32.9%	36.0%	80.6%
(B+A+GO)	90.0%↑	38.4%↓	96.2%	49.0%↑	34.0%↓	68.9%↓
(B+GO)+A	96.7%↑	98.3%↑	100.0%	48.9%↑	52.5%↑	80.9%
(A+GO)+B	35.0%↑	15.0%↓	98.0%	0.9%↓	2.3%↓	99.3%↑

3 A: Antibiotic (10 mg/L), B: Bacteria, GO: Graphene oxide(10 mg/L)

4
5

Table S4 Curve fitting results of XPS C 1s spectra

Peak	BE ^a (eV)	FWHM ^b (eV)	Area	%
C-C	284.66	1.52	41755.80	60.67
C-OH	286.08	1.20	2794.49	4.06
C=O	287.23	1.00	22077.28	32.08
O-C=O	288.97	0.50	2195.66	3.19

6 ^a Binding energy; ^b Full width at half-maximum, C:O=2.543

7
8

Table S5 Curve fitting results of XPS O 1s spectra.

Peak	BE (eV)	FWHM (eV)	Area	%
O-C=O	531.78	1.64	9488.98	17.09
C=O	532.96	1.47	33683.07	60.68
C-OH	533.53	1.74	12335.67	22.22

9